Journal of Power Sources 196 (2011) 8265–8271

Contents lists available at ScienceDirect

Journal of Power Sources

journal homepage: www.elsevier.com/locate/jpowsour

Enhancement of the fuel cell performance of a high temperature proton exchange membrane fuel cell running with titanium composite polybenzimidazole-based membranes

Justo Lobato*, Pablo Cañizares, Manuel A. Rodrigo, Diego Úbeda, F. Javier Pinar

Chemical Engineering Department, University of Castilla-La Mancha, Enrique Costa Building, Av. Camilo Jose Cela, n 12, E-13071 Ciudad Real, Spain

ARTICLE INFO

Article history:
Received 2 November 2010
Received in revised form 27 April 2011
Accepted 3 June 2011
Available online 13 June 2011

Keywords:
Composite
Durability
High temperature PEMFC
TiO_2
Performance
Polybenzimidazole

ABSTRACT

The fuel cell performance of a composite PBI-based membrane with TiO_2 has been studied. The behaviour of the membrane has been evaluated by comparison with the fuel cell performance of other PBI-based membranes, all of which were cast from the same polymer with the same molecular weight. The PBI composite membrane incorporating TiO_2 showed the best performance and reached 1000 mW cm^{-2} at 175 °C. Moreover, this new titanium composite PBI-based membrane also showed the best stability during the preliminary long-term test under our operation conditions. Thus, the slope of the increase in the ohmic resistance of the composite membrane was 0.041 mΩ cm^2 h^{-1} and this is five times lower than that of the standard PBI membrane. The increased stability was due to the high phosphoric acid retention capacity – as confirmed during leaching tests, in which the Ti-based composite PBI membrane retained 5 mol of H_3PO_4/PBI r.u. whereas the PBI standard membrane only retained 1 mol H_3PO_4/PBI r.u. Taking into account the results obtained in this study, the TiO_2–PBI based membranes are good candidates as electrolytes for high temperature PEMFCs.

1. Introduction

Polybenzimidazoles (PBIs) are a well-known class of polymers that have applications as high temperature matrix resins, non-flammable textile fibres, adhesives and foams [1]. Wainright et al. were the first to use a PBI–phosphoric acid complex as an electrolyte in high temperature proton exchange fuel cells (HT-PEMFCs) [2]. Since then, PBI has received increasing attention for this application. For example, in 2000 only ~25 manuscripts were published on this material whereas in 2008 the number increased to more than 250 manuscripts and more than 6000 citations, as reported recently by Li et al. [3].

The most desirable feature for the PBI to be an electrolyte in HT-PEMFC is its proton conductivity, which depends on the amount of phosphoric acid retained, i.e. the doping level [4,5]. The conductivity increases as the doping level increases, but the membranes lose mechanical strength. An optimum doping level must therefore be found for the proper operation of the fuel cell. The structure of PBI has been modified to improve its properties (conductivity, mechanical strength, etc.) either by modifying the monomer prior to polymerisation, by post-functionalisation of the polymer or by the addition of inorganic fillers. Inorganic fillers are typically added to increase the proton conductivity and/or acid uptake of PBI films. A number of methods for filling, blending and sulphonating PBI have been developed and were reviewed by Kerres [6]. As examples, phosphoric acid-doped PBI membranes have been incorporated with zirconium phosphate [7], phosphotungstic acid [7,8] and silicotungstic acid [9].

In the work described here, several types of PBI-based membranes for high temperature PEMFCs cast from the same polymer (with the same molecular weight) were prepared and tested in a single high temperature PEM fuel cell in order to compare the results and assess the benefits of adding TiO_2 particles. Thus, standard PBI, sulphonated PBI and titanium oxide composite PBI-based membranes were prepared. It should be noted that this paper is complementary to another one published by our group where the physicochemical characterization is discussed in greater depth [10]. The data presented in this work mainly concern the fuel cell performance and the potential use of these new composite membranes in an HT-PEMFC. TiO_2 has previously been used in Nafion-based composites [11,12] but not with PBI membranes. Leaching tests were carried out on the prepared membranes and the mechanical properties were assessed. Moreover, a preliminary long-term cell test (120 h) was carried out on the four different membranes and impedance analyses were performed to evaluate the results.

* Corresponding author. Tel.: +34 926 29 53 00x6707; fax: +34 926 29 52 56.
E-mail address: Justo.Lobato@uclm.es (J. Lobato).

0378-7753/$ – see front matter © 2011 Elsevier B.V. All rights reserved.
doi:10.1016/j.jpowsour.2011.06.011

2. Experimental

2.1. PBI membrane preparation

The PBI polymer was synthesised according to a procedure described elsewhere [13]. Different PBI-based membranes were prepared using a polymer with the same molecular weight. The chemicals were used as received. A chemically sulphonated PBI (sPBI) was synthesised as follows. Firstly, a standard PBI membrane was prepared using N,N-dimethylacetamide (DMAc) (99% purity, Panreac, Spain) as solvent (4.7 wt%) [13,14] and a film applicator with a doctor blade (Elcometer, S.A.) was used to cast the membrane. The solvent was removed as described in [14]. The standard PBI membrane was then sulphonated (s-PBI) according to the method described in a previous publication and the degree of sulphonation achieved was 84.8% (mol HSO_3/repeat unit PBI) [10]. The sPBI was made with the aim of obtaining PBI-based membranes with high conductivity. Moreover, membranes were directly cast using trifluoroacetic acid (TFA) (99% purity, Panreac, Spain) as solvent and doped with the desired amount of phosphoric acid to obtain 10 mol H_3PO_4/urPBI, which is similar to that the level achieved in the standard PBI membrane immersed in a bath of 85% H_3PO_4 [14]. The direct cast technique is based on the use of a solution of PBI and phosphoric acid in one phase. This approach allows the preparation of a doped membrane that is ready to use in a cell once the membrane is cast and the solvent is removed. Regarding the TiO_2 composite PBI-based membranes, these materials were prepared by the direct addition of titanium dioxide particles (Merck, mean particle size 1.14 μm) to a solution of PBI (2.2 wt%) in DMAc. A calculated amount of TiO_2 to obtain 2 wt% of TiO_2 in the membrane was added and the mixture was stirred in an ultrasonic bath for 2 h at room temperature to give a homogeneous solution. Finally, the membrane was cast by following the same procedure as for the standard PBI membranes [13,14]. The PBI solution used to prepare the TiO_2 composite PBI-based membrane had a lower concentration than the solution used to prepare the standard PBI membrane. This change was made to improve the dispersion of TiO_2 particles in the PBI solution.

Once the membranes had been prepared, all but the one prepared with TFA as solvent were immersed in phosphoric acid (85 wt%, Panreac, Spain) at room temperature to dope them.

The acid doping level and the water absorbed in the different membranes were calculated on the basis of thermogravimetric analysis. Two portions of the same PBI membrane were prepared with the same thickness and dimensions. Firstly, the membrane portions were introduced into an oven at 110 °C for 3–4 h to remove superficial water. The membranes were then weighed. Subsequently, one sample was dipped into a phosphoric acid solution of known concentration and the other portion was used for thermogravimetric analysis. For all the membranes studied, a weight loss was observed up to approximately 150 °C [10]. The weight loss was due to the loss of absorbed water from the membrane. Accordingly, this first analysis gave the weight percentage of water contained in the undoped PBI membrane, with the remainder being the polymer content. The second portion of membrane was immersed in the acid solution for at least five days, because this immersion time ensures that the membrane adsorbs the highest quantity of acid and the acid impregnation process is complete [14]. The membrane was removed from the phosphoric acid solution and the excess acid was wiped from the surface. The membrane portion was weighed and analysed by TGA. In this analysis a weight loss up to 150 °C was also observed but an additional weight loss process was evident above this temperature due to H_3PO_4 auto-polymerisation [10]. The second weight loss ranged from 150 °C to the end of the analysis. Hence, the second TGA allowed the levels of absorbed acid and water in the phosphoric acid-doped membrane to be calculated, taking into account the results (PBI amount) obtained in the first TGA. The calculation of acid and water absorption by the membranes was carried out using Eqs. (2.1) and (2.2):

$$\text{Adsorbed acid (mol } H_3PO_4\text{/r.u.PBI)} = \frac{(W_{\text{PBI+Acid, 2}} - W_{\text{PBI, 1}})/M_{w,\ H_3PO_4}}{W_{\text{PBI, 1}}/\text{r.u. PBI}} \quad (2.1)$$

$$\text{Adsorbed water (mol } H_2O\text{/r.u.PBI)} = \frac{(W_{\text{Water, 2}} - W_{\text{PBI, 1}})/M_{w,\ H_2O}}{W_{\text{PBI, 1}}/\text{r.u. PBI}} \quad (2.2)$$

where $W_{\text{PBI + Acid, 2}}$ is the weight of PBI and acid obtained from the second portion in the TGA; $W_{\text{PBI, 1}}$ is the weight of PBI obtained from the first portion; $W_{\text{Water, 2}}$ is the weight of water from the second portion; $M_{w,\ \text{H3PO4}}$ is the molecular weight of phosphoric acid; $M_{w,\ \text{H2O}}$ is the molecular weight of water; r.u. PBI is the repeat unit of PBI (308 g/r.u. PBI).

Table 1
Doping level reached after immersion of the membranes in a bath of 85% phosphoric acid (except for the membrane cast with TFA), water uptake and molar ratio of PBI/water of the PBI membranes prepared in this work.

Membrane	PBI	Sulphonated	Composite-TiO_2
Doping level (mol H_3PO_4/r.u. PBI)	11.3	15.3	15.3
Water uptake (mol H_2O/r.u. PBI)	11.6	22.3	17.5

The doping level and the amount of absorbed water in the different membranes prepared in this work are given in Table 1. The TGA data were obtained from a previous study, in which the physicochemical characterization is discussed in more detail [10]. The data in this table allow a better understanding of the fuel cell performance.

2.2. Physicochemical characterization

TGA analyses were performed on a Perkin-Elmer TGA7 Thermogravimetric Analyzer equipped with a Gas Selector and a TAC7/DX Thermal Analysis Controller. The samples were heated up from 25 °C to 550 °C at 10 °C min^{-1} under a nitrogen flow.

The leaching tests were carried out by washing the doped membranes in water at 80 °C for 2 h (until complete removal of the free acid) and the removed phosphoric acid, which was in the washing water, was measured by inductively couple plasma (ICP) analysis. Mechanical analyses were carried out on stress–strain curves obtained with a universal testing machine (Instron-5565) at 125 °C and 50% humidity and the crosshead speed was set at 5 mm min^{-1}.

2.3. Fuel cell assembly and testing

Fuel cell tests were performed in a cell consisting of two monopolar plates made of graphite impregnated with a phenolic resin (Sofacel, Spain) onto which flow fields with a serpentine geometry were machined. Heat was provided by means of heating rods inserted into the cell. The temperature of the system was regulated by a temperature controller (CAL 3300, Cal Controls Ltd., United Kingdom) connected to a thermocouple imbedded in the graphite blocks. Gold-plated metallic bolts were screwed into the blocks to allow electrical contact. Pure hydrogen and oxygen were fed at atmospheric pressure into the cell at a constant flow rate of 0.134 l min^{-1} and 0.076 l min^{-1}, respectively, without any additional pre-treatment.

For the preparation of the membrane–electrode-assemblies (MEAs), Toray graphite paper (TGPH-120, 10% wet-proofed, Etek Inc., USA) was used as the gas diffusion and supporting layer taking into account previous results [15]. A catalytic ink composed of 40% Pt on carbon black (Vulcan XC-72, Etek Inc., USA) [16], PBI as binder and DMAc as solvent was sprayed (using as carrier gas N_2) onto the graphite paper. The electrodes were then soaked with a 1 wt% H_3PO_4 solution (≈30 mg cm^{-2}) in order to make the PBI a proton conductor and to soften the contact between the membrane and

the electrodes. The Pt loading on both electrodes was 0.5 mg cm^{-2} and a C/PBI wt ratio of 20 was used on the basis of previous results [16,17]. The MEA preparation procedure concluded with the assembly of the electrodes and the membrane by hot-pressing. In this process the MEA was introduced between two stainless steel blocks equipped with heating rods and a temperature control system. Hot-pressing was performed at 130 °C by applying a load of 1 tonne for 15 min. The active area of the electrodes was 4.65 cm^2.

The electrochemical analysis was carried out by obtaining polarization curves and impedance spectra as follows. Firstly, the cell was kept at a constant temperature (125 °C) for 24 h, with the voltage monitored at a constant current density of 0.215 A cm^{-2} (1 A) with an Autolab PGSTAT30 potentiostat/galvanostat (Ecochimie, The Netherlands). In all cases, the cell voltage reached a stationary value. Polarization curves were obtained at different temperatures with a scan rate of 1 mV s^{-1} and a step potential of 1 mV. Impedance Spectra (IS) were obtained at a potential of 0.6 V under the different fuel cell conditions. The frequency ranged from 10 kHz down to 100 mHz, with a potential wave of 10 mV rms.

3. Results and discussion

3.1. Fuel cell tests

Fig. 1 shows the polarization curves at 125 (Fig. 1a), 150 (Fig. 1b) and 175 °C (Fig. 1c) for the different membranes studied in this work. In all cases, and as expected, the fuel cell performance improved with temperature due to the enhancement of the kinetic and diffusion processes [14,17,18]. At low current densities, i.e. the region governed by the oxygen reduction reaction (ORR), the voltage drop experienced by the cell was lower on increasing the temperature due to the enhancement of the ORR. In addition, at intermediate current densities – i.e. the region governed by the ohmic drop, which is responsible for the proton mobility – the slope of the *j*–*V* curves decreased as the temperature increased for all the membranes studied. Therefore, the improvement in these two factors combined with the decrease in the mass transfer problems led to an increase in the limiting current density (high current density region) on increasing the operating temperature. The worst performances were obtained with the standard PBI membrane and the one cast and doped directly, most likely due to the lower acid-doped content of these membranes. Moreover, at the three temperatures studied, the best yield was obtained with the titanium PBI-based composite, with a maximum power density of 1000 mW cm^{-2} at 175 °C, i.e. approximately 15% higher than that reached by the sulphonated membrane and approximately 45% higher with respect to the other membranes under the same conditions.

It can also be observed that the temperature has a marked influence on the fuel cell performance when the sulphonated membrane is used. Thus, at 175 °C the sulphonated membrane performed better than the standard membrane and the one doped and cast directly, whereas at 125 °C the sulphonated membrane gave the worst performance.

In order to gain a better understanding of the fuel cell responses and in order to split the different contributions of the cell overvoltages to the global response, performances were fitted to the following equations [19–22]:

$$E = E_0 - b \cdot \log \quad j - R \cdot j + b \cdot \ln\left(1 - \frac{j}{j_{\lim}}\right) \tag{3.1}$$

where

$$E_0 = E_r + b \cdot \log j_0 \tag{3.2}$$

where E_r (mV) is the reversible potential, b (mV dec^{-1}) is the Tafel slope (related to the kinetic overvoltage) and j_0 (mA cm^{-2}) is the exchange current density for the oxygen reduction reaction. Therefore, E_0 (mV) is the reversible potential and the contribution of the mixed potential of the oxygen electrode and the low rate of hydrogen crossover to the cathode (open circuit potential). j (mA cm^{-2}) is the current density, R (Ω cm^2) is the ohmic drop and $j_{\lim}$ is the limiting current density, related to the diffusion overvoltage (mA cm^{-2}). The values of these parameters are reported in Table 2.

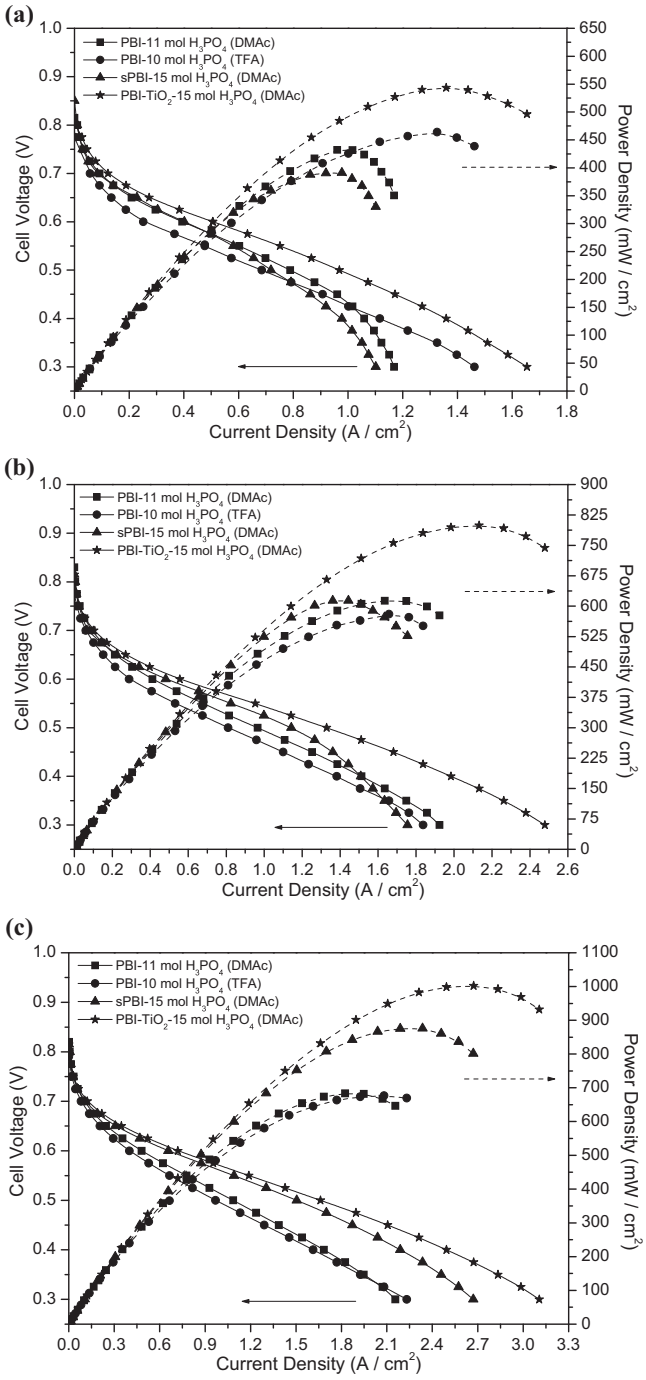

Fig. 1. Fuel cell performance (polarization, solid symbols and lines; power, open symbols and dashed lines) for different membranes. Atmospheric pressure. Pt load = 0.5 mg cm^{-2} in both electrodes. (a) T = 125 °C; (b) T = 150 °C; (c) T = 175 °C.

It can be stated that the open circuit potential is very similar for all of the samples, as are the Tafel slopes, because the electrodes prepared for all of the samples were the same. In contrast, the fitting of the internal resistance was different for each sample, with a lower internal resistance obtained on increasing the acid

Table 2
Characteristic fitted parameters of the polarization curves at $T = 175\,^{\circ}C$.

Sample	Open circuit potential, E_0 (mV)	Tafel slope, b (mV dec^{-1})	Internal resistance, R (mΩ cm^2)	Limiting current density, j_{lim} (mA cm^{-2})
PBI	868 ± 3	79 ± 1.5	81 ± 3	2687 ± 37
PBI (direct acid casting)	856 ± 5	79 ± 2.6	102 ± 7	3998 ± 445
sPBI	853 ± 3	71 ± 1.5	52 ± 2	2920 ± 14
2% TiO_2-PBI	840 ± 3	64 ± 2	58 ± 2	3490 ± 25

doping level. Finally, the cells with the worst performance showed lower limiting current densities, although this did not occur for the directly doped membrane. This fact indicates that mass transfer processes occur more rapidly in the TiO_2 composite PBI-based membrane fuel cell. In case of the directly doped membrane, the fitting error of the limiting current density was very high. However, this parameter is not significative, as in polarisation curves (Fig. 1c) no mass transfer limitations appeared.

Cell measurements were accompanied by an evaluation of the ohmic contribution. It is well known that the fuel cell resistance comes primarily from the ionic (electrolyte, membrane in this case) component [23]. Taking into account that only the membrane was changed between experiments, it can be assumed that the differences in the fuel cell resistance are due to the different conductivities of the membranes tested in this work. The conductivity values (calculated from the total ohmic resistance of the fuel cell) at the three temperatures studied are shown in Fig. 2. It can be seen that the conductivity increases with temperature. In all cases, the modified PBI membranes (sulphonated and titanium-based composite membranes) gave the highest values. This finding could be due to the higher doping levels achieved in these membranes. The difference between the standard PBI membranes and the modified ones became more marked on increasing the temperature. This fact could explain the very good performance of the sulphonated membrane at 175 °C. As pointed out in a previous publication by our group [24], and more recently by Daletou et al. [25], the water plays an important role in the conductivity mechanism and hence in the fuel cell performance. As indicated in Section 2, the modified membranes not only attained a higher acid doping level but also a higher water content, especially in the case of the sulphonated one. This means that at the highest temperature, where the availability of water is low due to dehydration processes [16], the sulphonated membrane is better at retaining the small amount of water available and thus performs better than the standard PBI membranes. The performance of this sulphonated PBI membrane is very interesting and is better than those shown by other sulphonated PBI membranes prepared by the same or similar procedures, where the sulphonated PBI showed low conductivities and hence low fuel cell performance [9,26]. These low performance levels could be ascribed to the fact that the membranes were poorly doped with phosphoric acid and therefore their conductivities were low.

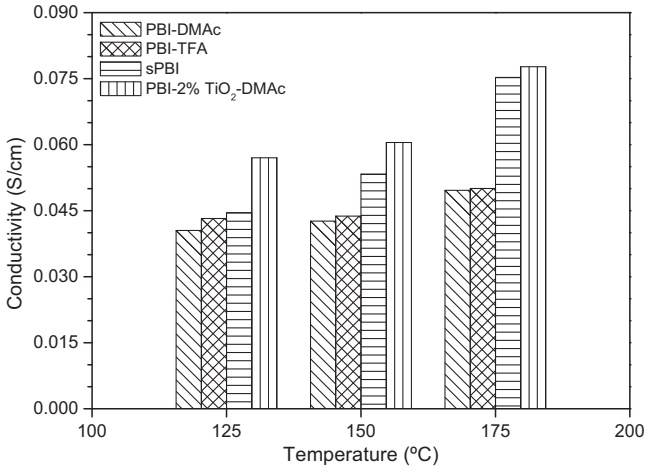

Fig. 2. Conductivities from the ohmic resistance of the cells at different temperatures.

3.2. Mechanical properties

It is known that for the acid-doped PBI membranes, high doping levels lead to high proton conductivity values, whereas the mechanical properties weaken at high doping levels. The tensile strength was calculated from the ultimate tensile stress at which the membrane sample broke. The mechanical properties of the different membranes tested in this work at 125 °C are shown in Table 3. A high tensile strength can be observed for the PBI membrane and this is related to the high molecular weight of the PBI polymer synthesised in this work (385.6 kDa). Thus, in this work a tensile strength of 446.0 MPa was obtained, which is higher than the 150 MPa at 125 °C previously reported for a pristine PBI membrane from a lower average molecular weight (25 kDa) [27]. In a previous work [13] a value of 120 MPa was determined for a weight-average molecular weight of 105.1 kDa, but this was measured at 25 °C. These results indicate the importance of the molecular weight on the mechanical properties, as reported previously [13,24], and show that the polymer used in this work has a high molecular weight, leading to robust mechanical properties of the subsequently cast membranes. Nevertheless, when the membrane is doped, the tensile strength decreases due to the plasticizing effect of the acid [28]. The modified membranes (sulphonated and titanium composite membranes) therefore showed the lowest tensile strength values. Highly doped membranes have shown high tensile strengths, i.e. in the range from 1 to 3.5 MPa [29,30]. Therefore, the low values of 2.9 MPa for the sulphonated membrane and 6.4 MPa for the titanium one can be considered as acceptable values to cast membranes for fuel operation at high temperatures. It can be seen from the data in Table 3 that the pristine PBI membrane showed an elongation at maximum stress of 40%, which is similar to values obtained for other PBI-based membranes. In contrast, all of the phosphoric acid-doped PBI membranes showed elongation values higher than 200%, indicating that both doped membranes become more plastic at high acid doping levels, i.e. the polymer chains are more flexible and can rearrange under load [24]. In the case of the membrane prepared by the direct acid cast method, this showed an elongation value close to that of the pristine PBI, which means that these kinds of membranes are less flexible than the others and

Table 3
Mechanical properties of different PBI-based membranes studied in this work.

Sample	Maximum stress (MPa)	Elongation (%)
PBI	446.0	40.1
PBI·11H_3PO_4	22.2	289.8
PBI·10H_3PO_4 *	58.2	70.6
sPBI·15H_3PO_4 (sulphonated membrane)	2.9	211.0
PBI–TiO_2·15H_3PO_4 (composite membrane)	6.4	224.9

* Direct acid casting with TFA.

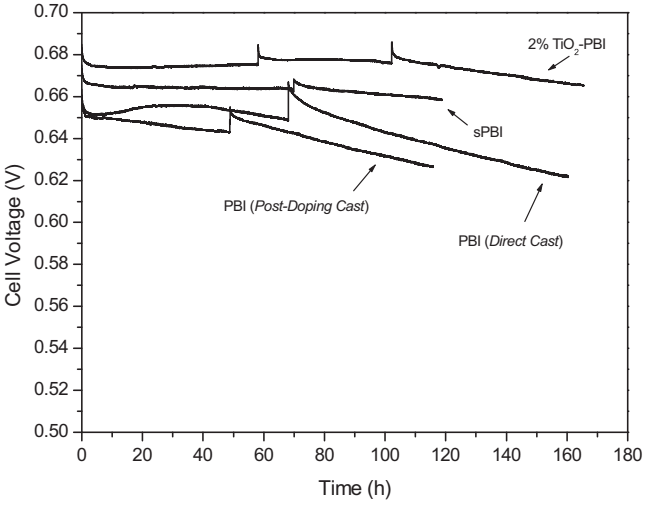

Fig. 3. Long-term durability test. $T = 175\,^{\circ}C$; $j = 0.215\,A\,cm^{-2}$ at atmospheric pressure.

also that the cast method influences the mechanical properties. For instance, property ranges from 0.27 to 2.24 MPa for tensile stress and 23–230% for elongation at break have been reported for a new generation of sulphonated PBI membranes [31].

3.3. Durability test

Once the fuel cell conditioning, polarization curve measurements and impedance spectroscopy studies had been performed, a preliminary long-term MEA performance durability test was carried out on the different PBI-based membranes prepared in this work. The membranes were operated at 175 °C without any humidification of either H_2 or O_2. The applied current density was $0.2\,A\,cm^{-2}$ for approximately 5 days. The voltage drop during the long-term test is represented in Fig. 3. A slight drop of the voltage throughout the long-term test can be seen for all the membranes, but the standard PBI and the direct cast membranes showed the highest decays. The titanium-based composite membrane showed the best performance, as one would expect, taking into account the polarization curves. Moreover, this membrane showed the best stability. The slope of the different cell voltage variations was calculated in order to estimate the voltage drop with time (115 h) and the following values were obtained: $-194.2\,\mu V\,h^{-1}$, $-107.6\,\mu V\,h^{-1}$, $-43.7\,\mu V\,h^{-1}$ and $+35.1\,\mu V\,h^{-1}$ for the standard PBI, the direct acid cast membrane, the sulphonated PBI membrane and the titanium composite membrane, respectively. Indeed, in the case of the titanium-based membrane it can be seen that the voltage increased. This demonstrates the good stability of this membrane during the first 115 h of operation. It is clear that the standard PBI membrane and the one acid-cast directly with TFA are far from the requirements needed for long-term operation. In contrast, the sulphonated PBI membrane and the titanium composite membrane show voltage decay rates within the range of others reported in literature [32]. For PBI-based membranes values of $-14\,\mu V\,h^{-1}$ and $-250\,\mu V\,h^{-1}$ have been reported recently [33]. Finally, a transient signal can be seen in all cases and this corresponds to the times at which the cell test was stopped and the activity was then resumed. Throughout the first few minutes, it seems that the cell recovers [33] but then suffers a large decay in the first few hours up to a certain voltage value. This final voltage value matches the normal drop of the cell voltage.

In order to gain a better understanding of the behaviour of the MEAs prepared with the different membranes during this stability test, impedance analyses were carried out at different operation

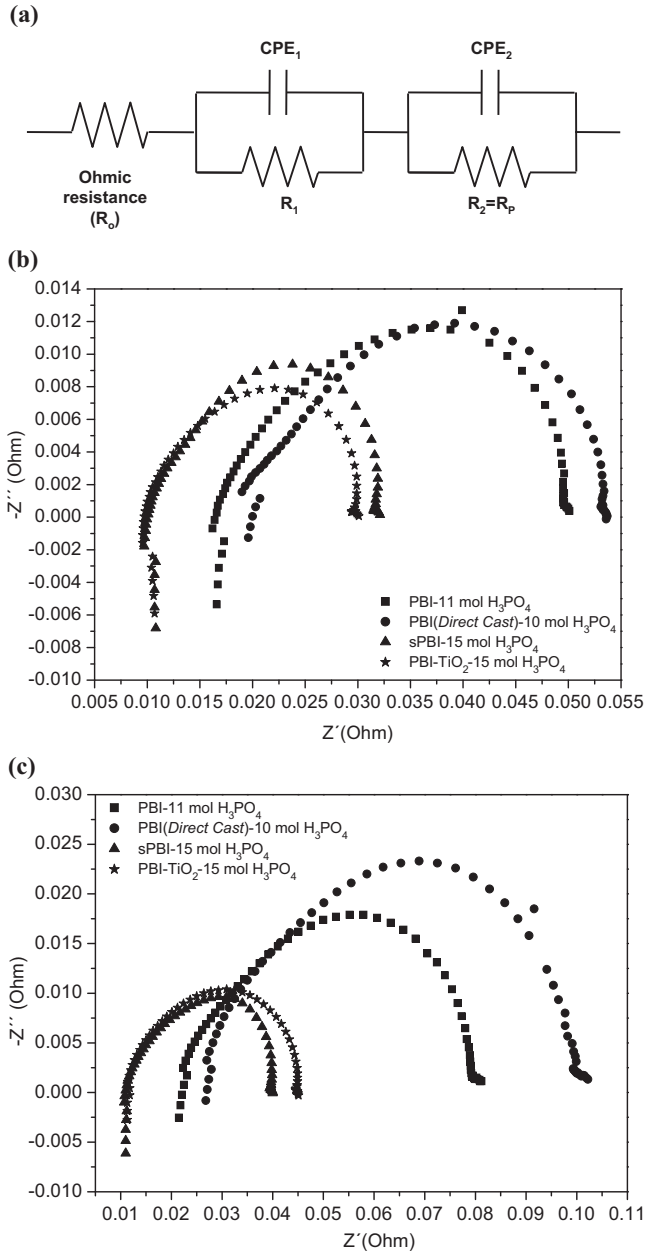

Fig. 4. Impedance spectroscopy analysis of the different membranes studied in this work. (a) Equivalent circuit used in this study; (b) Nyquist plots at the beginning and (c) at the end of the preliminary long-term test.

times. The corresponding Nyquist plots for the different membranes prepared in this work are shown in Fig. 4 at the beginning and at the end of the test. The equivalent circuit used to simulate the impedance data in this work, which were taken from the literature [16,17,34–38], are represented in Fig. 4. All of the spectra show a similar pattern, with a large semicircle and a quasi-imperceptible another one at the lowest frequencies. Moreover, in the case of the most resistive systems, a very small distorted arc appears at high frequencies. From high to low frequency, the first arc, according to Springer et al. [37] and Paganin et al. [38], stems from the distributed resistance effects in the electrolyte within the catalyst and this is not related to faradaic processes. The second and largest semicircle is related to the polarization of the electrode [39] and this is the process that controls the cell performance at this cell volt-

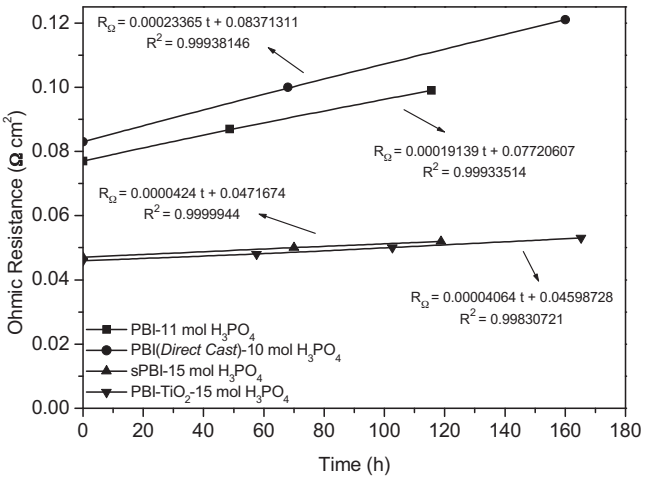

Fig. 5. Variation of the ohmic resistance with time during the preliminary long-term study.

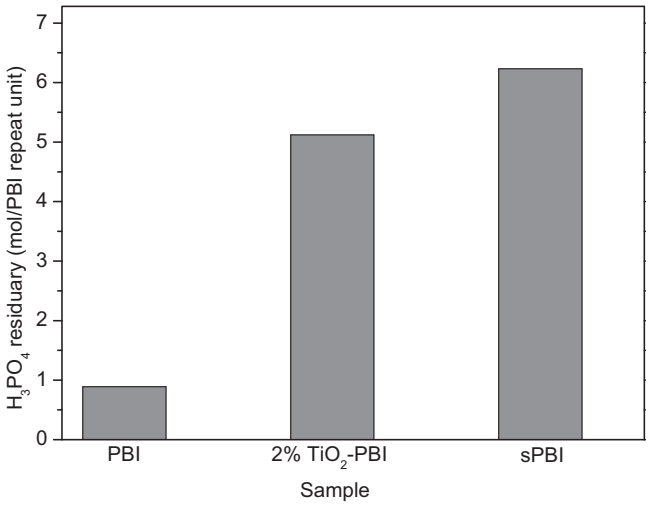

Fig. 6. Acid retained by the membranes after the leaching test.

age. Finally, the last small semicircle may be related to some kind of mass transfer limitations [36–39]. This semicircle appears for all the MEAs prepared and it can be explained in terms of the large amount of phosphoric acid contained in the membranes. According to Oono et al. [36], an excessive amount of phosphoric acid does not favour mass transfer processes. Oxygen transport in phosphoric acid is very limited [40]. However, this excess of phosphoric acid may help to enlarge the three-phase-boundary, accounting for the superior performance of some of the MEAs and, concomitantly, the slower ohmic resistance. For the purpose of this paper, attention will be mainly paid to the ohmic resistance and, to a lesser extent, the total resistance.

The variation of the ohmic resistance with time is shown in Fig. 5. Polarization, total resistances, the ratio between the ohmic resistance and total resistance, and the rate of increase of the polarization resistance are given in Table 4. A linear increase in the ohmic resistance with time can be observed in Fig. 5. The ohmic resistance represents around 30% of the total resistance, as can be seen from the data in Table 4. Taking into account the values of the slopes for the increase in the ohmic resistance (see Fig. 5: 0.191 mΩ cm^2 h^{-1}, 0.234 mΩ cm^2 h^{-1}, 0.042 mΩ cm^2 h^{-1} and 0.041 mΩ cm^2 h^{-1} for the standard PBI, the direct acid cast membrane, the sulphonated PBI membrane and the titanium composite membrane, respectively) and the corresponding slopes for the rate of increase of the polarization resistance (see Table 4), it can be concluded that the drop in the fuel cell performance is due, to a great extent, to the degradation of the electrode rather than to degradation of the membrane. This situation is especially visible in the case of TiO_2-based membrane.

The lowest increase in the ohmic resistance was shown by the sulphonated and composite PBI membranes, as can be verified in Fig. 5. It has been reported for PBI-based PEM fuel cells that the most likely mechanisms of membrane degradation involve the attack of H_2O_2 and peroxyl radicals (·OH or ·OOH) along with acid leaching [3,41]. It can therefore be suggested that the sulphonated and titanium composite membranes degrade more slowly than the standard PBI membranes studied in this work. In addition, these PBI-modified membranes may somehow contribute to decrease the catalyst sintering, catalyst dissolution and/or the corrosion of the carbon support, which are other primary causes of electrode degradation in PBI-based membranes for high temperature PEM fuel cells [3,41,42]. In the case of TiO_2, the presence of this material at the membrane–electrode interface (which provides the maximum contribution to the catalytic activity [18]) may have a similar effect to ZrO_2, as reported by Liu et al. [43].

3.4. Leaching test

As discussed above, one of the factors that contributes to the degradation of the PBI-based membranes is leaching of the doping acid (phosphoric acid), which is one the bottlenecks for the technological application of this kind of PEMFC. Several authors have observed and measured the acid leaching of PBI-based membranes during long-term tests [33,44], but in this work this loss was not

Table 4
Values of the resistance at different times for the different membranes prepared in this work.

Sample	Time (h)	Polarization resistance, R_{pol} (Ω cm^2)	Total resistance, R_{tot} (Ω cm^2)	R_Ω/R_{tot}	R_{pol} slope (mΩ cm^2 h^{-1})
PBI·11H_3PO_4	0	0.098	0.222	0.347	
	49	0.162	0.300	0.290	0.933
	115	0.207	0.372	0.267	
PBI·10H_3PO_4*	0	0.130	0.249	0.334	
	68	0.200	0.343	0.292	0.916
	160	0.278	0.468	0.258	
sPBI·15H_3PO_4 (sulphonated membrane)	0	0.019	0.147	0.321	
	70	0.032	0.175	0.287	0.158
	119	0.037	0.184	0.284	
PBI–TiO_2·15H_3PO_4 (composite membrane)	0	0.024	0.137	0.335	
	58	0.036	0.165	0.294	0.082
	103	0.036	0.170	0.296	
	165	0.039	0.206	0.255	

* Direct acid casting with TFA.

evaluated. In order to gain an insight into the acid retention capability of the new titanium composite membranes, leaching tests were carried out on the different membranes prepared in this work.

The acid that remained on the membrane after the leaching tests is represented in Fig. 6. The amount of acid remaining in the membranes was calculated by subtracting the acid leached from the membranes (data obtained from the washing water in which the membranes were washed in order to remove the acid absorbed and measured by ICP) from the results in Table 1 (acid absorbed by the membranes). It can be observed that the sulphonated PBI membrane retained the most phosphoric acid and this was followed by the titanium composite membrane. The standard PBI membrane lost almost all of the doped acid. These results confirm the good behaviour of the titanium composite membrane and explain why this type of membrane showed the best performance during the durability test, thus making it an interesting composite material for high temperature PEMFC.

4. Conclusions

In this work, four different PBI-based membranes with high doping levels (>10 mol H_3PO_4) were prepared. All of the membranes were cast from PBI with the same molecular weight and were tested in a high temperature fuel cell.

The composite PBI-based membrane with TiO_2 gave the best performance at the three different temperatures tested and also showed the best stability under the operating conditions. Thus, it has been demonstrated that the addition of TiO_2 to PBI-based membranes has a positive effect because it leads not only to a higher amount of phosphoric acid but also to enhanced acid retention, which is an important issue in this type of membrane.

Further work is currently underway in our laboratory aimed at optimising the amount of titanium and to gain a better understanding of composite PBI-based membranes using different titanium-based compounds.

Acknowledgements

The authors thank the JCCM (Junta de Comunidades de Castilla-La Mancha) and the enterprise CLM-H2 for financial support through Project PBI08-151-2045 and to MCINN (Ministerio de Ciencia e Innovación, Spain) for the fellowship AP2007-02713 awarded to D. Úbeda and financial support through the Project CTM2007-60472.

References

[1] J. Mader, L. Xiao, T.J. Schmidt, B.C. Benicewicz, Adv. Polym. Sci. 216 (2008) 63.
[2] J.S. Wainright, J.T. Wang, R.F. Savinell, M.H. Litt, J. Electrochem. Soc. 142 (1995) L121.
[3] Q. Li, J.O. Jensen, R.F. Savinell, N.J. Bjerrum, Prog. Polym. Sci. 34 (2009) 449.
[4] R. Bouchet, E. Siebert, Solid State Ionics 118 (1999) 287.
[5] Q. Li, H.A. Hjuler, N.J. Bjerrum, J. Membr. Sci. 31 (2001) 773.
[6] J.A. Kerres, Fuel Cells 5 (2005) 230.
[7] R.H. He, Q. Li, G. Xiao, N.J. Bjerrum, J. Membr. Sci. 226 (2003) 169.
[8] P. Staiti, M. Minutoli, S. Hocevar, J. Power Sources 90 (2000) 231.
[9] P. Staiti, M. Minutoli, J. Power Sources 94 (2001) 9.
[10] J. Lobato, P. Cañizares, M.A. Rodrigo, F.J. Pinar, J. Membr. Sci. 369 (2011) 105.
[11] E.I. Santiago, R.A. Isidoro, M.A. Dresch, B.R. Matos, M. Linardi, F.C. Fonseca, Electrochim. Acta 54 (2009) 4111.
[12] Z.G. Shao, H. Xu, M. Li, I.-M. Hsing, Solid State Ionics 177 (2006) 779.
[13] J. Lobato, P. Cañizares, M.A. Rodrigo, J.J. Linares, J.A. Aguilar, J. Membr. Sci. 306 (2007) 47.
[14] J. Lobato, P. Cañizares, M.A. Rodrigo, J.J. Linares, G. Manjavacas, J. Membr. Sci. 280 (2006) 351.
[15] J. Lobato, P. Cañizares, M.A. Rodrigo, C. Ruiz-López, J.J. Linares, J. Appl. Electrochem. 38 (2008) 793.
[16] J. Lobato, P. Cañizares, M.A. Rodrigo, J.J. Linares, D. Úbeda, F.J. Pinar, Fuel Cells 10 (2010) 312.
[17] J. Lobato, P. Cañizares, M.A. Rodrigo, J.J. Linares, F.J. Pinar, Int. J. Hydrogen Energy 35 (2010) 1347.
[18] F. Seland, T. Berning, B. Børrensen, R. Tunold, J. Power Sources 160 (2006) 27.
[19] J. Lobato, P. Cañizares, M.A. Rodrigo, J.J. Linares, R. López-Vizcaíno, Energy Fuels 22 (2008) 3335–3345.
[20] P. Argyropoulos, K. Scott, A.K. Shukla, C. Jackson, J. Power Sources 123 (2003) 190–199.
[21] J. Lobato, P. Cañizares, M.A. Rodrigo, J.J. Linares, Fuel Cells 5 (2009) 597–604.
[22] S. Srinivasan, Fuel Cells: From Fundamentals to Applications, Springer Science + Business Media, New York, 2006.
[23] R. OïHayre, S.-W. Cha, W. Colella, F.B. Prinz, Fuel Cell Fundamentals, John Wiley & Sons Inc., New York, 2006.
[24] J. Lobato, P. Cañizares, M.A. Rodrigo, J.J. Linares, Electrochim. Acta 52 (2007) 3910.
[25] M.K. Daletou, J.K. Kallitis, G. Voyiatzis, S.G. Neophytides, J. Membr. Sci. 326 (2009) 76.
[26] M.J. Ariza, D.J. Jones, J. Roziere, Desalination 147 (2002) 183.
[27] R. He, Q. Li, A. Bach, J.O. Jensen, N.J. Bjerrum, J. Membr. Sci. 277 (2006) 38.
[28] Q.F. Li, H.C. Rudbeck, A. Chromik, J.O. Jensen, C. Pan, T. Steenberg, M. Calverley, N.J. Bjerrum, J. Kerres, J. Membr. Sci. 347 (2010) 260.
[29] L.X. Xiao, H.F. Zhang, E. Scanlon, L.S. Ramanathan, E.W. Choe, D. Rogers, T. Apple, B.C. Benicewicz, Chem. Mater. 17 (2005) 5328.
[30] L.X. Xiao, H.F. Zhang, T. Jana, E. Scanlon, R. Chen, E.W. Choe, L.S. Ramanathan, S. Yu, B.C. Benicewicz, Fuel Cells 5 (2005) 287.
[31] J.A. Mader, B.C. Benicewicz, Macromolecules 43 (2010) 6706.
[32] F.A. de Brujin, V.A.T. Dam, G.J.M. Janssen, Fuel Cells 1 (2008) 3.
[33] S. Yu, L. Xiao, B.C. Benicewicz, Fuel Cells 3–4 (2008) 165.
[34] J. Zhang, Y. Tang, C. Song, J. Zhang, J. Power Sources 172 (2007) 163.
[35] X. Yuan, H. Wang, J.C. Sun, J. Zhang, Int. J. Hydrogen Energy 32 (2007) 4365.
[36] Y. Oono, A. Sounai, M. Hori, J. Power Sources 189 (2009) 943.
[37] T.E. Springer, T.A. Zawodzinski, M.S. Wilson, S. Gottesfeld, J. Electrochem. Soc. 143 (1996) 587.
[38] V.A. Paganin, C.L.F. Oliveira, E.A. Ticianelli, T.E. Springer, E.R. Gonzalez, Electrochim. Acta 43 (1998) 3761.
[39] N.H. Jalani, M. Ramani, K. Ohlsson, S. Buelte, G. Pacifico, R. Pollard, R. Staudt, R. Datta, J. Power Sources 160 (2006) 1096.
[40] D. Chu, Electrochim. Acta 43 (1998) 3711.
[41] R. Borup, J. Meyers, B. Pivovar, Y.S. Kim, R. Mukundan, N. Garland, D. Myers, M. Wilson, F. Garzon, D. Wood, P. Zelenay, K. More, K. Stroh, T. Zawodzinski, J. Boncella, J.E. McGrath, M. Inaba, K. Miyatake, M. Hori, K. Ota, Z. Ogumi, S. Miyata, A. Nishikata, Z. Siroma, Y. Uchimoto, K. Yasuda, K. Kimijima, N. Iwashita, Chem. Rev. 107 (2007) 3904.
[42] Y. Zhai, H. Zhang, G. Liu, J. Hu, B. Yi, J. Electrochem. Soc. 154 (2007) B72.
[43] G. Liu, H. Zhang, Y. Zhai, Y. Zhang, D. Xu, Z.-G. Shao, Electrochem. Commun. 9 (2007) 135.
[44] C. Wannek, B. Kohnen, H.F. Oetjen, H. Lippert, J. Mergel, Fuel Cells 8 (2008) 87.